Thermal activation of vortex motion in $YBa_2Cu_3O_{7-\delta}$ films at low temperatures

B. M. Lairson, J. Z. Sun,* T. H. Geballe,† M. R. Beasley,† and J. C. Bravman
Department of Materials Science and Engineering, Stanford University, Stanford, California 94305
(Received 1 October 1990)

Thermally activated flux vortex motion in a constant applied field is studied at temperatures between 2.5 and 21 K for *in situ* thin films of $YBa_2Cu_3O_{7-\delta}$. The magnitude and temperature dependence of the dissipation is shown to be consistent with an activation energy $U(J)$, which is independent of temperature in this temperature region, but which is assumed to be a function only of current J. Activation energies $U(J)$ are deduced for currents between 1×10^7 and 2.5×10^7 A/cm^2 for the samples measured, by considering the change in the decay rate, at constant current, as a function of temperature. These results indicate that the fundamental mechanism for dissipation in this temperature range is thermally activated.

INTRODUCTION

Many models have been proposed for the detailed description of magnetic relaxation in high-temperature superconductors.[1–9] These models make different assumptions about which properties of high-T_c materials are most important in describing the critical current and I-V characteristics. For instance, the magnetic penetration depth, the coherence length, the degree of anisotropy, and weak coupling between layers have all been considered. One feature which distinguishes some of these models from others is the assumption that thermally activated magnetic flux motion is responsible for the observed dissipation characteristics. For instance, Feigel'man *et al.*[2] argue that the flux creep activation energy $U(J)$ provides a description of the decay process, but that $U(J)$ is highly nonlinear in the current due to changes in the correlation volume with macroscopic current J. Fisher *et al.*[5] also argue that the observed dissipation is thermally activated, via thermal nucleation of flux vortex loops, although the appropriate activation energy must be described properly in terms of the H-T magnetic phase diagram.

Alternately, it has been proposed that the observed I-V characteristics and magnetic relaxation are the result of nonthermal effects. For instance, Lensink *et al.*[10] propose that magnetic relaxation at low temperatures is due to a nonthermal process, e.g., flux vortex tunneling. Recently,[11] some of the present authors have pointed out that an inhomogeneous critical-current distribution might be the dominant cause of dissipation observed in isothermal and magnetization decay over a wide temperature range, as has been observed in measurements of low-temperature superconductors.[12]

Here, for $YBa_2Cu_3O_{7-\delta}$ thin films, we investigate the question of thermally activated dissipation in detail for temperatures between 2.5 and 20 K. We postulate the existence of an approximately temperature-independent activation-energy barrier for flux vortex motion $\Delta F(J)$ in this temperature range. We deduce the function $\Delta F(J)$ from measurements of the relaxation rate of the current versus temperatures as described below.

EXPERIMENTAL

$YBa_2Cu_3O_{7-\delta}$ thin films were grown to a thickness of approximately 1.2 μm by off-axis magnetron sputtering, as described elsewhere.[13] The films were highly c-axis oriented, with a sharp transition temperature $T_{c0}=86$ K as removed from the deposition chamber.

Magnetization measurements were performed with the field parallel to the film surface normal on a modified Princeton Applied Research vibrating sample magnetometer. Using the Bean formula,[14] critical currents for the samples were determined to be 2.3×10^7 A/cm at 4.2 K in an applied field of 5 kG. We find the measured critical currents to be independent of thickness for films grown between 0.2 and 1.2 μm, indicating that the volume pinning force is not thickness dependent in this thickness range.

Magnetization decay measurements were made by ramping the field to a high value (11 kG) and then slowly ramping the field linearly in time down to 5.0 kG, where the ramping was stopped. This procedure saturated the observed moment throughout the measured temperature range. The magnetic moment was measured at 1 sec time increments for 1000 sec, starting a few seconds before the final field value was reached. Because measurements were made in an applied field substantially larger than the self-field if the samples, self-field effects were neglected.

THEORY OF MAGNETIZATION DECAY

Consider those magnetization states for which we can write the decay of the supercurrent R in a fixed applied field H_a as

$$R(J,T)=-dJ/dt\ . \tag{1}$$

That is, where the current decay rate deduced from the Bean formula is only a function of the temperature and the average current J as determined from the sample moment. States of this type include those reached by isothermal decay from the saturated moment at constant applied field (in magnetization decay), and those in which this process is followed by changing the temperature of

the sample.[13] Equation (1) does not apply for more complex distributions of the flux, for instance, those which arise if there is overshoot in the applied field at the end of the ramp.[15] The magnetic field dependence of R is implicit in Eq. (1), but is not included explicitly in order to simplify the notation below.

From Eq. (1) we can write

$$dR = \left[\frac{\partial R}{\partial J}\right]_T dJ + \left[\frac{\partial R}{\partial T}\right]_J dT \ , \tag{2}$$

and by the chain rule,

$$\left[\frac{\partial R}{\partial J}\right]_T \left[\frac{\partial J}{\partial T}\right]_R \left[\frac{\partial T}{\partial R}\right]_J = -1 \ . \tag{3}$$

The three quantities on the left are experimentally accessible from, respectively, isothermal decay or I-V measurements, from critical current versus temperature measurements, and from cooling measurements at constant current.[13] The second factor on the left can be taken as J_c versus T, since a fixed decay rate corresponds to a constant electric field, from Faraday's law. Equation (3) establishes that, for those situations for which Eq. (1) holds, only two of these three types of measurements can be treated as being independent.

Model for thermal activation

One general model for describing decay processes assumes thermally activated relaxation. This assumption specifies that the decay rate can be written

$$R(J,T) = \gamma(J,T)\exp[-\Delta F(J,T)/kT] \ , \tag{4}$$

where γ is a prefactor proportional to some attempt frequency and length scale, while $\Delta F(J,T)$ is a free-energy difference between the minimum and activated states. Note that the assumption of thermal activation in Eq. (4) does not place a limitation on the mechanism for the thermally activated dissipation. For instance, Eq. (4) does not select between glassy behavior and Anderson flux creep, since both of these models assume that the dissipation is thermally activated.[1,5] We make the assumption that the primary temperature dependence in Eq. (4) is through the exponent, while the prefactor γ only depends on the current J. Various generalizations of Eq. (4) can be made based on additional assumptions about the system. One generalization is allowing a range of energy barriers to flux motion, such that the right-hand side becomes a sum;[6] another is the introduction of inhomogeneous regions of the sample which possess different I-V curves at constant temperature, as illustrated by Fig. 5 in Ref. 11. Here, we do not consider generalizations of this form. Instead, we investigate quantitatively the degree to which a single pinning function $\Delta F(J,T)$ can describe observed decay without the use of these additional parametrizations.

If we switch free variables from T to $1/T$ and R to lnR, which are more convenient quantities for using Eq. (4), we can write from Eqs. (2) and (4) that

$$\left[\frac{\partial \ln R}{\partial J}\right]_T = \left[\frac{d\ln\gamma(J)}{dJ} - \frac{1}{kT}\left[\frac{\partial \Delta F(J,T)}{\partial J}\right]_T\right] \tag{5}$$

and

$$\left[\frac{\partial \ln R}{\partial (1/T)}\right]_J = \frac{-\Delta F(J,T)}{k} + \frac{T}{k}\left[\frac{\partial \Delta F(J,T)}{\partial T}\right]_J \ . \tag{6}$$

In terms of a thermally activated dissipation process, Eq. (5) is applicable to isothermal decay and I-V measurements, and Eq. (6) is appropriate for describing the case where the sample is cooled at constant J, as described below.

The second term on the right-hand side of Eq. (6) can be neglected at low temperatures relative to the first term. The quantity $\Delta F(J,T)$ is expected to become relatively constant versus temperature at low temperatures, since we associate it with the condensation energy of the superconductor. At low temperature ($T < 0.2T_c$), Eq. (6) therefore yields a more or less direct measurement of the pinning activation barrier $\Delta F(J)$. Consistent with common usage,[1,7] hereafter we use the symbol U to denote free energy. We denote the experimental activation barrier deduced from experimental data using Eq. (6) as $U^{**}(J)$.

Different forms for $U(J)$ can be constructed based on different physical assumptions.[1,2,7] For illustration, we show one such functional form in Fig. 1, which is a pinning function of the form

$$U(J) = U_p\left[1 - \frac{J}{J_c}\right]^n \ , \tag{7}$$

where U_p is the depth of the pinning well in the presence of no macroscopic current and J_c is the current at which

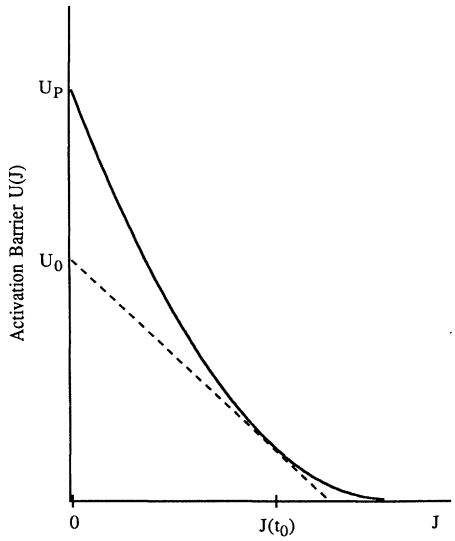

FIG. 1. Schematic vortex pinning potential showing approximate construction for U_0. U_p is expected to be finite for Anderson flux creep.

no barrier to flux flow exists. The exponent n depends sensitively on the shape of the potential well. Typically, for simple Anderson flux creep models, $1<n<2$.[1,7] Different physical assumptions, of course, lead to different functional forms for the activation potential, for example, $U(J)\propto J^{-(1/\mu)}$, where μ is a parameter.[2,5]

We now discuss measured magnetization decay data in terms of Eqs. (1)–(6). We consider whether thermally activated dissipation described by a single pinning potential adequately describes the decay process in the measured temperature range.

Historically, isothermal decay of the magnetization has been used extensively to determine energy U_0. U_0 is a geometric construct obtained from $U(J)$ at some particular value of J by extrapolating $(dU/dJ)_T$ linearly back to the $J=0$ origin, with $U(J)\ll U_0$ assumed.[1] Failure of this assumption introduces uncertainty into the calculated intercept, and precludes the simple calculation of a flux bundle volume. The construction of U_0 is indicated by the dashed line in Fig. 1. If the total current decay in the experimental region probed is very small, then the pinning potential, for instance Eq. (7), can be expanded to first order in J, about its value at some time during the measurement t_0, with γ assumed to be constant relative to changes in U.[1] This yields a decay solution of supercurrent J versus time t approximately

$$J(t)=J_0-kT\left[\frac{\partial J}{\partial U}\right]_0\ln(t/t_0)\ , \tag{8}$$

where J_0 is the value of the supercurrent at time t_0. This expression can be made more complicated by considering the initial condition in the magnetization decay experiment[15,16] or the breakdown of flux creep at large values of J,[6] but it contains the important features for the present discussion. The subscript indicates some nominal time during the course of the experiment, about which a time expansion is taken. The coefficient of the logarithmic time decay term can be used to calculate an energy intercept U_0. Usual values for U_0 in conventional superconductors are $U_0\approx 150kT$, so the linearization procedure and the assumption $U_0\gg U$ is satisfactory, where U is assumed to be of order of a few kT.

In high-T_c superconductors, the observed decays are rather large. This requires that we reevaluate our linearization procedure and our assumption about the size of U_0. A simple consideration of a model potential, for example Eq. (7), quickly reveals that a linearized potential is inadequate over the range of current decay (20%) which is typical in magnetization decay experiments, in that $(\partial U/\partial J)_T$ varies considerably over this range of decay. Therefore, strictly logarithmic decay will not be obtained for cases where the total decay is large, except when $n=1$. Further, the assumption that $U(J)\ll U_0$ also becomes invalid for large relaxations. For high-T_c materials, U_0 is extrapolated to be $(20-60)kT$.[17,18] In a typical decay over three orders of magnitude in time, say between 1 sec and 1000 sec, $U(J)$ increases by $\sim 6kT$. Typically, one extrapolates back to phonon frequencies to estimate when $U=0$, i.e., 10^{-10} sec.[6] This yields values for U of $\sim 20kT$ at experimentally accessible times, which are comparable to U_0.

These considerations do not affect the general applicability of the flux creep model, nor should the failure of a system to obey Eq. (8) necessarily be taken as a failure of the Anderson flux creep model without consideration of the magnitudes of the various quantities involved, such as the total decay which occurs during the course of the experiment.

Equation (8) results from the imposition of a locally linear pinning potential function in the neighborhood of a current J_0. Here, we develop a more general isothermal decay equation which takes into account the first nonlinear term in the pinning potential $U(J)$, also expanded about the current J_0 occurring at time t_0:

$$U(J)\approx U(J_0)+\left[\frac{\partial U}{\partial J}\right]_0(J-J_0)+\frac{1}{2}\left[\frac{\partial^2 U}{\partial J^2}\right]_0(J-J_0)^2\ . \tag{9}$$

This is the potential assumed by Beasley *et al.*,[1] with the addition of an additional term in the Taylor expansion to explicitly consider nonlinearity in the pinning potential. Again, we assume that changes in γ are relatively small, and obtain the following approximate expression for the isothermal magnetization decay in the neighborhood of t_0:

$$J(t)=J_0-kT\left[\frac{\partial J}{\partial U}\right]_0\ln(t/t_0)+\frac{(kT)^2}{2}\left[\frac{\partial J}{\partial U}\right]_0^3\left[\frac{\partial^2 U}{\partial J^2}\right]_0\ln^2(t/t_0)\ . \tag{10}$$

We define the quantities α and β for parametrizing experimental data:

$$J(t)=J_0-\frac{kT}{\alpha}\ln(t/t_0)+\frac{(kT)^2}{2}\frac{\beta}{\alpha^3}\ln^2(t/t_0)\ . \tag{11}$$

α and β are therefore the experimentally determined values for the first and second derivatives of the pinning potential with respect to the current, respectively, obtained from fits to isothermal decay data using Eq. (11). α is the same quantity in Eq. (8) which is customarily used to determine U_0.

The effect of the nonlinearity in the pinning potential is to add an addition term to Eq. (10), which is quadratic in $\ln(t)$. Equation (10) does not result from the imposition of any additional assumptions on the flux creep model; rather it explicitly includes a term which previously has justifiably been neglected as small. Equation (10) can be used to extract values involving the pinning potential $U(J)$, by fitting to magnetization decay data.

RESULTS

We now consider the various types of data available experimentally, which consist of isothermal decay (I-V) measurements, J_c measurements, and constant J versus T decay rate measurements.

Isothermal decay

A straightforward experiment to perform is the observation of isothermal decay of the supercurrent in a constant applied magnetic field. Typically, the external field is ramped to a certain value, H_a, at constant temperature, and the magnetic moment of the sample is recorded as a function of time.

Figure 2 shows typical data of this type, for an applied field of 5 kG at a temperature of 20.4 K. The same data are plotted in Figs. 2(a)–(2c). In Fig. 2(a), a straight line has been drawn approximately parallel to the data to illustrate the fit of Eq. (8) and to illustrate the nonlogarithmic behavior of the decay. An alternate type of fitting, based on a fixed power n in the I-V characteristic,[3,13] also does not yield an exact fit to the data, as illustrated in Fig. 2(b); however, it does provide a better fit than the logarithmic fit of Fig. 2(a). (A small vertical offset has been made to the dashed curves to clarify the illustration.) It is found experimentally that the departures from fits of the type shown in Figs. 2(a) and 2(b) increase for increasing temperature.

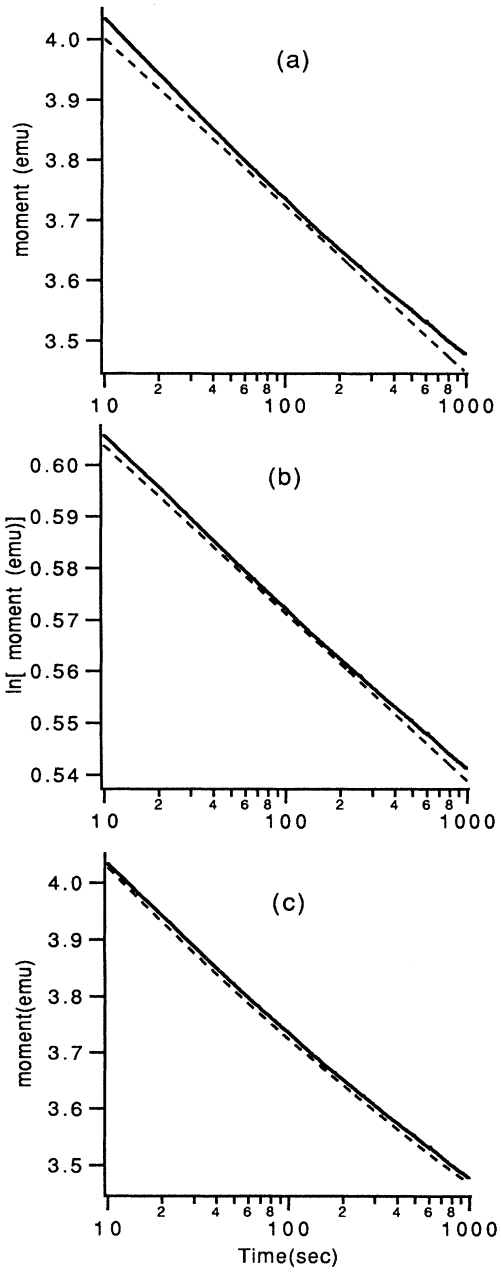

FIG. 2. Fit of measured isothermal magnetic decay data (solid line) to various I-V characteristics. (a) Exponential [Eq. (8)], (b) power law, (c) second-order exponential [Eq. (11)].

If we assume that the pinning potential is a nonlinear function of the macroscopic current, we can fit the data using Eq. (10), as illustrated in Fig. 2(c). With the appropriately chosen values for the first and second derivatives of the pinning potential, the quality of the fit is apparent. Data obtained at higher temperature, for instance 77 K, are also well described using this procedure.

The use of Eq. (10) allows an additional fitting parameter to be employed, so improvement in the fits is not surprising. We now attempt to verify that the fits obtained are consistent with a nonlinear pinning potential. We do this by considering the temperature dependence of the magnetization decays. If we assume that at low temperature the pinning function $U(J,T)$ reduces approximately to a temperature-independent form $U(J)$, then we can compare the quantities α and β by taking the discrete derivative of the slope of the pinning potential determined at two different temperatures, i.e.,

$$\left.\frac{\delta\alpha}{\delta J}\right|_0 = \frac{\alpha(T_1,J_1)-\alpha(T_2,J_2)}{J_1-J_2} \ . \tag{12}$$

The subscript "0" in Eq. (12) denotes that we take the discrete derivative using values for $\alpha(J,T)$ at some fixed time in the decay measurement, for instance 30 sec after stopping the field ramp. The subscript to J denotes the value of current measured at time t_0 at the two different temperatures.

If the model of thermal activation with a nonlinear $U(J)$ is correct, we then expect that

$$\left.\frac{\delta\alpha}{\delta J}\right|_0 \approx \beta \ , \tag{13}$$

i.e., that the curvature of the pinning potential determined from the two different methods, one at constant temperature, the other at constant time, will yield comparable values.

Figure 3 illustrates the values for the curvature of the pinning function derived in the two fashions, for data taken between 3.2 and 20 K. The dots represent the discrete derivatives of α from Eq. (12), while the squares denote values for β, from Eq. (10).

As can be seen in the plot, Eq. (13) holds rather well over this data range. This supports the notion that the nonlogarithmic behavior in the magnetization decay is due to a nonlinearity in the pinning potential.

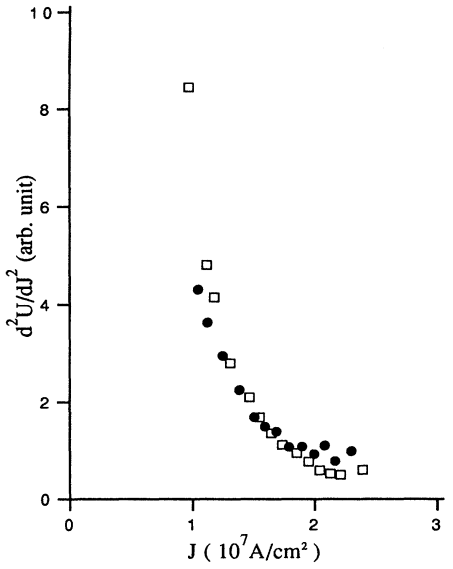

FIG. 3. Comparison of β (open squares) and $d\alpha/dJ$ (solid circles) vs current.

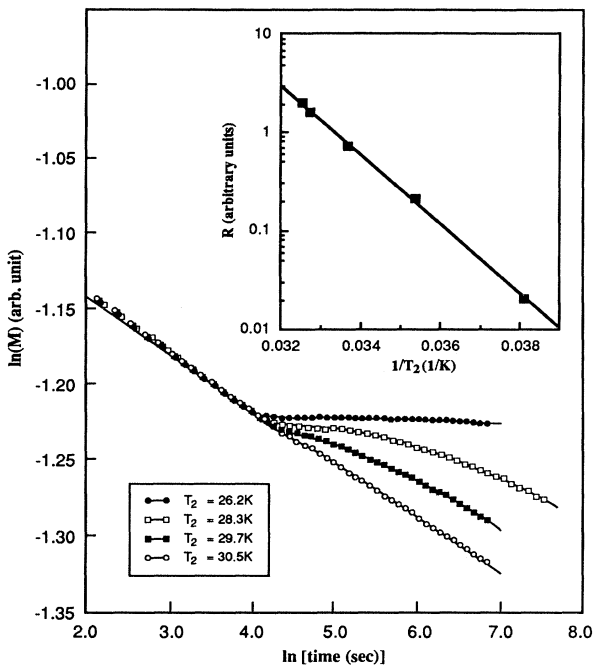

FIG. 4. Sample moment vs time for a sample cooled to various temperatures T_2 at $t_1 \sim 55$ sec. Solid lines represent best-fit values, shown in the inset, using a power-law form [illustrated in Fig. 2(b)]. Inset: Decay rate R vs T_2. Solid line represents a best fit to an Arrhenius expression $\ln R \propto 1/T$.

Rate versus temperature for a fixed current

In this experiment, the sample is cycled at constant field ramp rate to a fixed value of applied field H_a at constant temperature T_1. The sample is allowed to decay at this field value to some subsequent time, t_1, just as in the isothermal decay experiment above. At time t_1, the temperature is changed to a new temperature T_2. The decay of the sample moment is observed constantly during this process.

We assume that the sample is brought to the same initial state at t_1 each time the process above is repeated. If we assume that the process by which dissipation occurs is by the motion of flux vortices in the sample, then the significant effect of the temperature change from T_1 to T_2 is on the average velocity of the flux vortices, as observed by a change in the rate at which the moment of the sample decays.

Typical data of this form are shown in Fig. 4, which shows magnetization decay data in which the sample temperature was reduced at $t_1 \approx 55$ sec, from an initial temperature $T_0 = 30.7$ K in an applied field of 5.07 kG. The figure consists of the superposition of four decay experiments, for which $T_2 = 30.5$ K, $T_2 = 29.7$ K, $T_2 = 28.3$ K, and $T_2 = 26.2$ K. The solid lines are fits of using a power law I-V relationship to parametrize the decay rate subsequent to the cool, as has been discussed elsewhere.[3,13]

If we assume that the vortex motion is thermally activated, then the change in the decay rate should be approximately described by an Arrhenius expression, where the rate varies exponentially with inverse temperature. The inset to Fig. 4 shows the best-fit decay rate versus $1/T_2$. The data shown in the inset are well described by an Arrhenius expression over two orders of magnitude in the decay, as indicated by the solid line fit. This yields a value of $U \approx 70$ meV.

The most notable features from Fig. 4 are, first, that the change in the decay rate does in fact appear to be Arrhenius in character, since the rate versus inverse temperature is approximately exponential; second, that the observed decay rates are the same as those which are expected when the state at (t_1, T_2, H_a) is reached by isothermal decay. This implies that we can perform the experiment illustrated by Fig. 4 by reaching the moment at t_1 by isothermal decays at various temperatures, which is a much easier experiment. These rates can then be used to construct $U(J,T)$ values using Arrhenius plots, so long as U is relatively constant over the range of temperature considered. In the Anderson flux creep model, it is most likely that the values of $U(J,T)$ have their smallest temperature dependence for $T \ll T_c$, since the activation energies in Eq. (4) are customarily associated with the free energy of a vortex in this case.[19]

We perform the experiment represented by Fig. 4, in the range $2.5\ \text{K} < T < 21$ K, by making isothermal decay measurements in temperature increments of 0.5–1 K. We then calculate best-fit values for $U(J)$ from Arrhenius plots, implicitly assuming that the temperature dependence is negligible in this temperature range. Generally, the data were well described by an Arrhenius expression using this procedure, although data in the neighborhood of 5–8 K yielded plots exhibiting a small positive curvature. Such curvature might signal the breakdown of one

or more of the assumptions made for obtaining activation energies in this fashion.

The resulting best-fit values for $U(J)$, denoted as $U^{**}(J)$, are shown in Fig. 5. Within the assumptions mentioned here, the points in this plot represent a direct measurement of the pinning potential of the superconductor versus the macroscopic current J, using a least-squares fit to Eq. (11). The solid line is a quadratic fit to the $U^{**}(J)$ data, shown for illustration. The pinning potential shown in Fig. 6 is intuitively reasonable, approaching zero as J increases and falling off roughly as a power law, with $n=2$.

One difference between the classical Anderson flux creep model and the vortex glass model is the value of the thermal activation energy as J approaches zero, which is finite for the classical Anderson model,[1,6,7] but diverges for the vortex glass model.[5] It is interesting to consider whether the potential versus J shown in Fig. 5 can address this question. Although the fit to Eq. (7) yields a finite intercept at $U_p \sim 100$ meV, it should be noted that the power law in J guarantees a finite intercept at $J=0$. Maley *et al.*[20] consider an experimentally determined function $U_e(J)$, which they find consistent with a form $U(J) \propto \ln(J_c/J)$. Such a form might be consistent with the onset of a vortex glass phase, as reported by Koch *et al.*,[21] in 0.3-μm-thick $YBa_2Cu_3O_{7-\delta}$ films. We find a fit to this form, which diverges as J approaches zero, also yields a qualitative fit to the data. It is therefore quite difficult to distinguish experimentally between a vortex glass and Anderson flux creep based simply on data of the form shown in Fig. 5.

A natural question is whether the pinning potential derived from the cooling at constant current, and the first derivative of the magnetization decay, yield consistent values for the pinning potential. We make this comparison, within the context of the foregoing assumptions, by

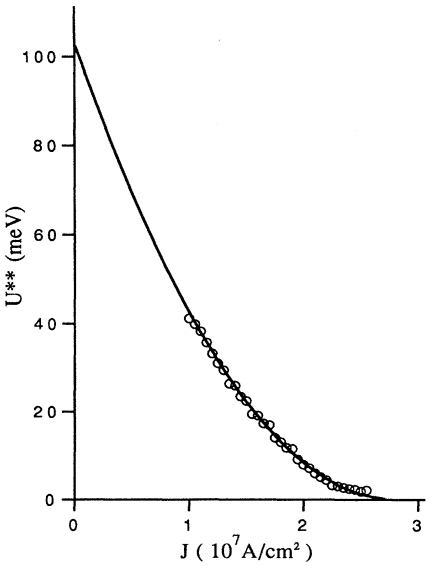

FIG. 5. Values of $U(J)$ determined from Arrhenius plots at constant current J.

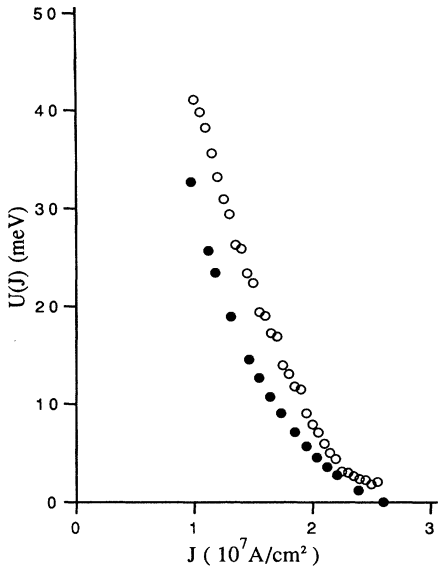

FIG. 6. Comparison of $U(J)$ determined from Arrhenius measurements (open circles) and from an integration of the isothermal decay measurements (solid circles). $U(J)$ is fixed at zero at $J=2.6\times10^7$ A/cm^2 for the integration.

performing a discrete integration of the pinning potential slopes $\alpha(J_i,T_i)$ determined from Eq. (11) at various temperature T_i. The subscript on J indexes the values of J_0 for different temperatures:

$$U_\alpha(J_m) \equiv U_\alpha(J_0) + \sum_{i=1}^{m} \alpha(J_i,T_i)(J_i - J_{i-1}) \ . \tag{14}$$

Here $U_\alpha(J)$ is the experimentally derived pinning potential obtained from the isothermal decay measurements. To fix a starting point for Eq. (14), we take $U=0$ at $J_0=2.6\times10^7$ A/cm^2, the highest current measured in the experiment. This procedure for calculating $U_\alpha(J)$ is essentially equivalent to that employed by Maley *et al.*[20] for finding $U_e(J)$, in which the isothermal relaxations are used to construct the nonlinear pinning potential.

Figure 6 shows the comparison between the resulting pinning potential derived from Eq. (14), i.e., isothermal decay data, and from Eq. (6). As can be seen in the figure, the agreement is relatively good. It is interesting to note, also, that the pinning potential constructed from the isothermal decays for our thin films (solid circles) appears similar to that constructed for oriented powders.[20]

Critical current versus temperature

As a final consideration of the consistency of a thermally activated flux motion model for the dissipation, we make a comparison between the temperature dependence of the critical current and pinning potential, similar to the comparison made by Tahara *et al.*[22] We can also consider the critical current versus temperature, which, with the previous assumptions, reduces to

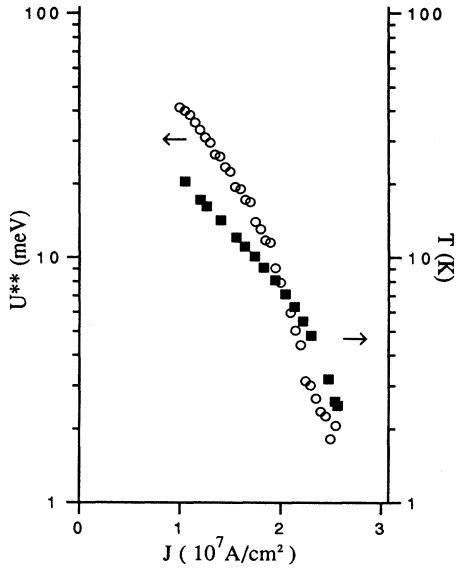

FIG. 7. Comparison of temperature vs J_c and pinning potential U^{**} vs J. The two curves should have comparable slopes, from Eq. (16).

$$\left[\frac{\partial J}{\partial(1/T)}\right]_R = \left[\frac{1}{kT}\left[\frac{\partial U(J,T)}{\partial J}\right]_T\right]^{-1}\left[\frac{U(J)}{k}\right]. \quad (15)$$

Note that we have already assigned measured quantities to the two terms on the right, in terms of the other two partials in Eq. (3). If we were to substitute these on the right-hand side, the relationship (15) would be tautological by virtue of Eq. (3).

If we again assume, in the temperature range $0 < T < 20$ K, that $U(J,T)$ is independent of temperature, then Eq. (15) becomes

$$\left[\frac{\partial J}{\partial \ln T}\right]_R = \left[\left[\frac{\partial \ln U(J,T)}{\partial J}\right]_T\right]^{-1}. \quad (16)$$

That is, the change in the critical current with the logarithm of temperature is equal to the change versus the logarithm of the pinning potential. Taking $U^{**}(J)$ in Fig. 5 for $U(J)$ on the right-hand side, and the value of J_c deduced for a constant applied field ramp on the left-hand side, we compare the two sides of Eq. (16). This is illustrated in Fig. 7.

As can be seen in the figure, the slopes of the two curves differ by approximately 50%. This can be taken again as qualitative agreement between the two measurements in terms of a simple flux creep picture.

CONCLUSIONS

Magnetization decay data have been interpreted in terms of thermally activated dissipation. It is found that the first and second derivatives of the magnetization decay versus $\ln(t)$, the critical current versus temperature, and isocurrent cooling experiments all give comparable values for the relevant quantities in the pinning potential, which is assumed to be only a function of the current in the temperature range $T < 20$ K. It is shown that, within the assumption of thermally activated flux creep, a measurement of $U(J)$ can be obtained at low temperatures from Arrhenius measurements of the magnetic relaxation rate at constant current. The level of agreement between the various measurements supports the notion that thermally activated flux motion in $YBa_2Cu_3O_{7-\delta}$ thin films is responsible for the bulk of the dissipation in the temperature range $2.5\ \text{K} < T < 20$ K.

The model of a single thermally activated pinning potential $U(J)$ does not preclude additional assumptions about the system, for instance, the presence of dissipation due to a multiplicity of decay paths with varying energy,[6] or the presence of inhomogeneities in the system which would complicate the decay of the system.[3,11] These represent generalizations of Eq. (4), which could presumably reconcile the differences in the pinning potential determined using the various methods, represented by Figs 3, 6, and 7. Conceptually, these generalizations are straightforward, although the analysis might be quite complicated for a specific set of assumptions.

ACKNOWLEDGMENTS

The authors would like to thank Dr. G. Deutscher and S. K. Streiffer for many helpful discussions. This work was supported by EPRI Contract RP8009-11, and the Standford Center of Materials Research supported under the NSF-MRL program.

*At Superconductor Technologies, Inc., Santa Barbara, CA 93111.

†At Department of Applied Physics, Stanford University, Stanford, CA 94305.

[1]M. R. Beasley, R. Labusch, and W. W. Webb, Phys. Rev. **181**, 682 (1969).

[2]M. V. Feigel'man, V. B. Geshkenbein, A. I. Larkin, and V. M. Vinokur, Phys. Rev. Lett. **63**, 2303 (1989); V. M. Vinokur, M. V. Feigel'man, V. B. Geshkenbein, and A. I. Larkin, *ibid.* **65**, 259 (1990).

[3]J. Z. Sun, B. M. Lairson, C. B. Eom, J. Bravman, and T. H. Geballe, Science **247**, 307 (1990).

[4]P. H. Kes, J. Aarts, J. van den Berg, C. J. van der Beek, and J. A. Mydosh, Supercond. Sci. Technol. **1**, 242 (1989).

[5]D. S. Fisher, M. P. A. Fisher, and D. A. Huse, Phys. Rev. B **43**, 130 (1991).

[6]C. W. Hagen, E. Salomons, R. Griessen, and B. Dam, Phys. Rev. Lett. **62**, 2857 (1989).

[7]Youwen Xu, M. Suenaga, A. R. Moodenbaugh, and D. O. Welch, Phys. Rev. B **40**, 10 882 (1989).

[8]T. Natterman, Phys. Rev. Lett. **64**, 2454 (1989).

[9]S. Doniach, Phys. Rev. B **41**, 6668 (1990).

[10]J. Lensink, C. F. J. Flipse, J. Roobeek, and R. Griessen, Physica C **162-164**, 663 (1989).

[11]J. Z. Sun, C. B. Eom, B. M. Lairson, J. C. Bravman, and T. H. Geballe, Phys. Rev. B **43**, 3002 (1991).

[12]W. H. Warnes, J. Appl. Phys. **63**, 1651 (1988).
[13]B. M. Lairson, J. Z. Sun, J. C. Bravman, and T. H. Geballe, Phys. Rev. B **42**, 1008 (1990).
[14]C. P. Bean, Phys. Rev. Lett. **8**, 250 (1962).
[15]R. Griessen, J. G. Lensink, T. A. M. Schroder, and B. Dam, Cryogenics **30**, 563 (1990).
[16]B. M. Lairson *et al.* (unpublished).
[17]J. Z. Sun, C. B. Eom, B. M. Lairson, J. C. Bravman, T. H. Geballe, and A. Kapitulnik, Physica C **162-164**, 687 (1989).
[18]L. Civale, A. D. Marwick, M. W. McElfresh, T. K. Worthington, A. P. Malozemoff, F. H. Holtzberg, J. R. Thomson, and M. A. Kirk, Phys. Rev. Lett. **65**, 1164 (1990).
[19]P. W. Anderson, Phys. Rev. Lett. **9**, 309 (1962).
[20]M. P. Maley, J. O. Willis, H. Lessure, and M. E. McHenry, Phys. Rev. B **42**, 2639 (1990).
[21]R. H. Koch, V. Foglietti, W. J. Gallagher, G. Koren, A. Gupta, and M. P. A. Fisher, Phys. Rev. Lett. **63**, 1511 (1989).
[22]S. Tahara, S. M. Anlage, J. Halbritter, C. B. Eom, D. K. Fork, T. H. Geballe, and M. R. Beasley, Phys. Rev. B **41**, 11 203 (1990).